

Article

# Manipulation of Si Doping Concentration for Modification of the Electric Field and Carrier Injection for AlGa<sub>N</sub>-Based Deep-Ultraviolet Light-Emitting Diodes

Mengqian Fang<sup>1,2</sup>, Kangkai Tian<sup>1,2</sup>, Chunshuang Chu<sup>1,2</sup>, Yonghui Zhang<sup>1,2</sup>,  
Zi-Hui Zhang<sup>1,2,\*</sup>  and Wengang Bi<sup>1,2,\*</sup> 

<sup>1</sup> Institute of Micro-Nano Photoelectron and Electromagnetic Technology Innovation, School of Electronics and Information Engineering, Hebei University of Technology, 5340 Xiping Road, Beichen District, Tianjin 300401, China; fmq48@hotmail.com (M.F.); tiankangkai24@hotmail.com (K.T.); chuchunshuang@hotmail.com (C.C.); zhangyh@hebut.edu.cn (Y.Z.)

<sup>2</sup> Key Laboratory of Electronic Materials and Devices of Tianjin, 5340 Xiping Road, Beichen District, Tianjin 300401, China

\* Correspondence: zh.zhang@hebut.edu.cn (Z.-H.Z.); wbi@hebut.edu.cn (W.B.);  
Tel.: +86-22-6043-5772 (Z.-H.Z.); +86-22-6043-5772 (W.B.)

Received: 19 May 2018; Accepted: 12 June 2018; Published: 20 June 2018



**Abstract:** Electron overflow is one of the key factors that limit the quantum efficiency for AlGa<sub>N</sub>-based deep-ultraviolet light-emitting diodes. In this work, we report a numerical study to improve the electron injection efficiency by manipulating the electric field profiles via doping the n-Al<sub>0.60</sub>Ga<sub>0.40</sub>N electron source layer with different concentrations and reveal the physical mechanism of the Si doping effect on the electron and the hole injection. By utilizing the appropriate doping concentration, the electric field will reduce the electron drift velocity and, thus, the mean free path. Therefore, a higher electron capture efficiency by the multiple quantum wells (MQWs) and an increase of the hole concentration in the active region can be realized, resulting in an improved radiative recombination rate and an optical output power.

**Keywords:** Si doping; depletion; electric field; electron mean free path; electron capture; carrier injection; deep-ultraviolet light-emitting diodes

## 1. Introduction

AlGa<sub>N</sub>-based deep-ultraviolet light-emitting diodes (DUV LEDs) have received considerable attention due to their promising applications in scopes, including air purification, water sterilization, biomedicine, ultraviolet (UV) curing, gas sensing, optical data storage, and communication [1]. However, DUV LEDs are still facing the challenge of low internal quantum efficiency (IQE), which is in the range of 50~80% and is obtained by low temperature photoluminescence measurement [2]. The IQE can be even lower if the device is electrically driven. As reported, the electron mobility is as high as ~500 cm<sup>2</sup>/Vs, which means electrons easily overflow from the MQW active region. The electron leakage causes low electron injection efficiency and is deemed as one of the main origins leading to the low IQE for DUV LEDs [3]. Therefore, it is required to reduce electron overflow. The electron leakage rate can be suppressed if more electrons are involved in the process of the radiative recombination with holes, which, however, can be achieved by increasing the hole injection efficiency [4], e.g., utilizing the p-type doped quantum barrier (QB) [5]. It is useful to reduce the electron accumulation at the interface between the last QB and the p-type electron blocking layer (p-EBL) by using the polarization self-screened

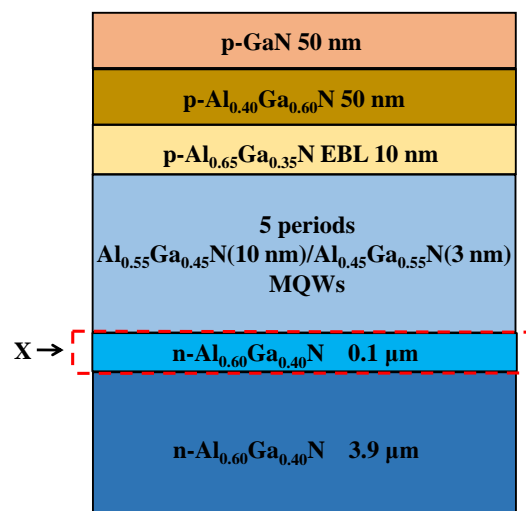
p-EBL [6] and the AlInGaN polarization matched p-EBL [7]. In addition, the superlattice p-EBL enables a good reflectivity for those electrons with high thermal energy, provided that the thickness of the superlattice structure is fully optimized [8,9]. In addition, designs of novel QB structures for DUV LEDs are proposed to increase the efficiency of electron injection, such as QBs with graded thickness [10] and thickened last QB with p-type doping [11]. Specifically, Guo et al. propose to insert a “spike” layer with even higher AlN composition in each AlGaN-based quantum barrier for DUV LEDs [12]. By doing so, the quantum wells can better capture the electrons, having reduced energy. The underlying mechanism for the proposed QB is that the polarization induced electric field in the “spike” Al-rich layer can reduce the kinetic energy for electrons, which, simultaneously, reduces the electron drift velocity and then decreases the electron mean free path. Next, the drift velocity for the free electrons can also be reduced by using an electron cooler (EC) or an n-type electron blocking layer [13,14]. Inspired by Refs. [12–14], we manipulate the electric field of the n-Al<sub>0.60</sub>Ga<sub>0.40</sub>N electron source layer by tuning the Si doping concentration [see Figure 1]. In this study, a very strong electric field can be generated if the Si doping concentration in the n-Al<sub>0.60</sub>Ga<sub>0.40</sub>N layer becomes high. Moreover, the generated electric field therein can decelerate the electrons and, hence, the electrons will become less mobile. As a result, the electron mean free path will become shorter and the electrons are more likely to fall into the MQWs, with a longer dwell time to more efficiently recombine with the holes. However, LEDs, with excessively higher Si doping concentrations, will, in turn, displace the recombination position and, therefore, hinder the hole injection, leading to an overall reduced radiative recombination rate [15]. Therefore, it is critical to design the DUV LEDs with an optimized Si doping level for maximizing both the carrier injection and the device performance. Subsequently, details will be given and discussed. Our work is different from the reports in Refs. [16,17]. Ryu et al. report that, by increasing the Si doping concentration for the n-GaN layer in GaN-based vertical blue LEDs, improved current spreading and more uniform carrier distribution in the quantum wells can be obtained [16]. Lee et al. report that the crystal quality for the [11–22] oriented n-GaN layer and the subsequent InGaN/GaN multiple quantum wells can be improved by properly increasing the Si doping concentration for the n-GaN layer. The reduced defect density in the n-GaN layers suppresses the carrier scattering and carrier mobility is, correspondingly, increased, which enables more efficient electron injection into the active region [17]. Therefore, this work reveals the impact of the Si dopants in increasing the DUV LED performance from another perspective.

## 2. Structures and Parameters

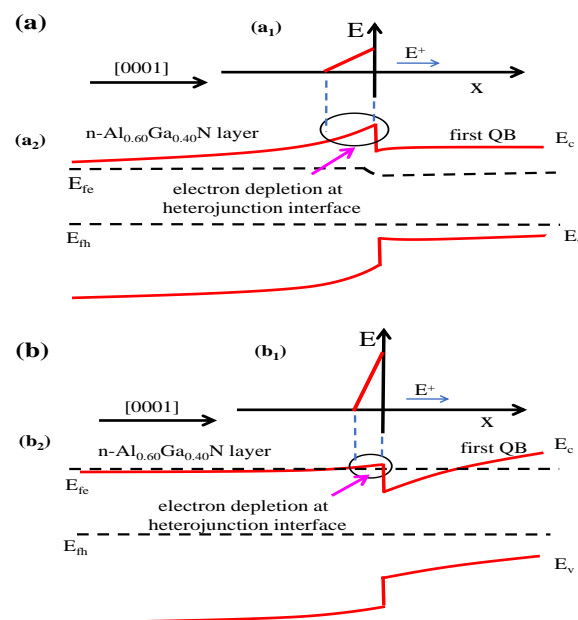
To reveal the impact of different Si doping concentrations on the electric field profile within the n-Al<sub>0.60</sub>Ga<sub>0.40</sub>N depletion region and the corresponding carrier injection efficiency, we designed DUV LED devices, as shown in Figure 1. The electron source layer was a 4 μm thick n-Al<sub>0.60</sub>Ga<sub>0.40</sub>N layer and the effective electron concentration was set to  $1.0 \times 10^{18} \text{ cm}^{-3}$ , except for the region labeled as “X region” in Figure 1. The X region has different Si doping concentrations for the DUV LEDs, i.e., the 0.1 μm thick X region had electron concentrations ranging from  $9.0 \times 10^{16} \text{ cm}^{-3}$  to  $4.0 \times 10^{20} \text{ cm}^{-3}$ . The active region for all three DUV LEDs contained five periods of Al<sub>0.45</sub>Ga<sub>0.55</sub>N/Al<sub>0.55</sub>Ga<sub>0.45</sub>N MQWs, with a well thickness and barrier thickness of 3 nm and 10 nm, respectively. Then, a 10 nm thick p-Al<sub>0.65</sub>Ga<sub>0.35</sub>N EBL, with the effective hole concentration of  $7.0 \times 10^{16} \text{ cm}^{-3}$ , was adopted on top of the MQWs. The p-EBL was then followed by a 50 nm thick p-type Al<sub>0.40</sub>Ga<sub>0.60</sub>N layer, with an effective hole concentration of  $9.0 \times 10^{16} \text{ cm}^{-3}$ . Lastly, a 50 nm thick p-GaN layer, with an effective hole concentration of  $1.0 \times 10^{17} \text{ cm}^{-3}$  was capped on the p-type Al<sub>0.40</sub>Ga<sub>0.60</sub>N layer. The mesa size for the three devices was set to  $350 \times 350 \mu\text{m}^2$ .

Figure 2 shows the underlying mechanism for manipulating the electric field in the n-Al<sub>0.60</sub>Ga<sub>0.40</sub>N layer. The electric field ( $E$ ) can be formulated by  $E = \sigma / \epsilon = N_{\text{dopant}} \cdot l_{\text{depletion}} / \epsilon$ , from which we know that the magnitude of the electric field ( $E$ ) is determined by the ionized donor concentration ( $N_{\text{dopant}}$ ), the width of the depletion region ( $l_{\text{depletion}}$ ), and the dielectric constant ( $\epsilon$ ). The product of  $N_{\text{dopant}}$  and  $l_{\text{depletion}}$  produces the sheet charge density ( $\sigma$ ). One can increase the electric field magnitude by increasing  $\sigma$  or reducing  $\epsilon$ . In this study, the AlN composition for the X region was unchanged, resulting in

a constant  $\epsilon$ . Hence, this work probes the impact of the Si doping concentration in the X region on the electric field magnitude. Once the Si doping concentration in the X region decreases, the value of  $l_{depletion}$  will become larger [see Figure 2a<sub>2</sub>]. On the other hand,  $l_{depletion}$  will decrease if the Si doping concentration in the X region increases [see Figure 2b<sub>2</sub>]. Considering the higher ionization energy for the Si dopants that are doped into the Al-rich n-Al<sub>0.60</sub>Ga<sub>0.40</sub>N layer, this work sets the effective Si doping concentration (i.e.,  $N_{dopant}$ ) within the range from  $9.0 \times 10^{16} \text{ cm}^{-3}$  to  $4.0 \times 10^{20} \text{ cm}^{-3}$ . Then, we attempted to identify a feasible way to increase the  $\sigma$  in this work.



**Figure 1.** Schematic architectural diagram for structures with different Si doping concentration in the n-Al<sub>0.60</sub>Ga<sub>0.40</sub>N layer.



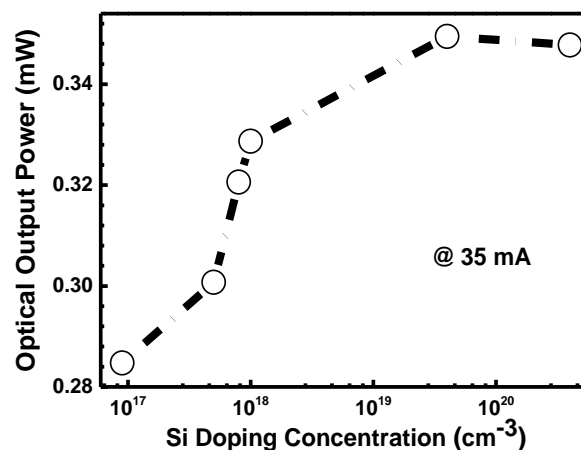
**Figure 2.** Schematic energy diagrams and electric field profiles within the heterojunction interface for the structures (a) with a low Si doping concentration in the X region and (b) with a high Si doping concentration in the X region.  $E_c$ ,  $E_v$ ,  $E_{fe}$ , and  $E_{fh}$  represent the conduction band, the valence band, the quasi-Fermi levels for electrons, and holes, respectively.

The numerical calculations were conducted by using Advanced Physical Models of Semiconductor Devices (APSYS). Firstly, the polarization level was set to 40% [18]. The Auger recombination coefficient

was set to  $1.0 \times 10^{-30} \text{ cm}^6\text{s}^{-1}$  [19] and the Shockley-Read-Hall (SRH) recombination lifetime in the MQWs was assumed to be 10 ns [19]. The energy band offset ratio for  $\text{Al}_x\text{Ga}_{1-x}\text{N}/\text{Al}_y\text{Ga}_{1-y}\text{N}$  heterojunction was set to 50/50 [20]. The electron effective mass for the AlGaN material was obtained by conducting linear extrapolation between the electron effective mass for the AlN material and the electron effective mass for the GaN material [21], and the calculated values for the effective electron mass were consistent with the report in Ref. [22]. Our calculation programs could solve Poisson's equation, Schrödinger equation, and the current-continuity equation self-consistently. Other parameters on nitrogen-containing III-V semiconductors can be found elsewhere [23].

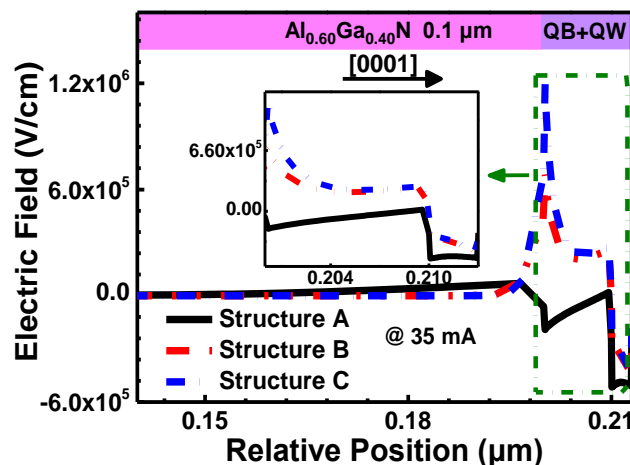
### 3. Results and Discussions

Figure 3 shows the optical output power for DUV LED structures with different Si doping concentrations in the X region, from which we can see that the optical output power first increases to a maxima and then decreases as the Si doping concentration level in the X region further increases. The improved optical power can be ascribed to the enhanced electron injection efficiency, which was caused by the modulated electric field and the reduced electron mean free path. However, with further increases of the Si doping concentration, the optical output power tended to decrease. The main reason for this is that the hole concentration in the MQWs was reduced. The origin of the carrier injection efficiency variation and the impact on the radiative recombination rate within the MQW region will be discussed subsequently. To better interpret the observations in Figure 3, we selectively doped the  $0.1 \mu\text{m}$  thick X region with  $9.0 \times 10^{16} \text{ cm}^{-3}$ ,  $4.0 \times 10^{19} \text{ cm}^{-3}$ , and  $4.0 \times 10^{20} \text{ cm}^{-3}$  for Structures A, B, and C, respectively.



**Figure 3.** Optical output power for DUV LED structures with different Si doping concentrations in the X region. Data are collected at the injection current level of 35 mA.

Figure 4 presents the electric field profiles in the X region and the first quantum barrier/quantum well (QB/QW) for Structures A, B, and C, respectively. We can find that the depletion region in the X region for Structure C was shorter than that for Structures A and B, which is ascribed to the larger Si doping concentration level. Note, the depletion layer in the X region for Structure A also completely lies in the  $0.1 \mu\text{m}$  thick X region. Meanwhile, the electric field intensity for Structure C was also the strongest among the three DUV LEDs and the electric field intensity in the X region for Structure A was the smallest. Therefore, from Figure 4, we can conclude that the electric field intensity in the X region can become high by increasing the Si doping concentration in the  $n\text{-Al}_{0.60}\text{Ga}_{0.40}\text{N}$  layer. Meanwhile, the electric field in the X region for all the three devices was directed to the [0001] orientation, which helps to reduce the kinetic energy and the drift velocity for the free electrons. By doing so, the quantum wells can capture the electrons more efficiently, leading to a reduced electron leakage level [12–14].



**Figure 4.** Electric field profiles in the n-Al<sub>0.60</sub>Ga<sub>0.40</sub>N layer and the first QB/QW for Structures A, B, and C, respectively, at the injection current of 35 mA.

By following the equation of  $W = \int_0^x q \times E(x) dx$ , the energy that the electrons lose ( $W$ ) for Structures A, B, and C can be obtained. Here,  $q$  represents the unite electronic charge and  $E(x)$  represents the electric field profiles that are shown in Figure 4 for the three investigated DUV LEDs. The integration range is denoted as  $x$ . By referring to the electric field profiles in Figure 4, the energy loss was calculated to be 150.61 meV for Structure A, 316.83 meV for Structure B, and 372.07 meV for Structure C. Therefore, the electron kinetic energy of structure C was the smallest and the electron deceleration effect for Structure C was the strongest. Consequently, the MQWs have the strongest ability to capture electrons [12–14], while the electron capture efficiency of the MQWs for Structure A is the lowest that will be shown subsequently.

Figure 5a shows that Structure C has the highest electron concentration and Structure A has the lowest electron concentration in the MQWs. The electron concentration agrees with the physical mechanism discussed earlier that the modulated electric field decelerates the electrons and then enhances the ability for the MQWs to capture electrons. It is questionable that the high Si doping concentration in the X region also contributes to the large electron concentration levels in the MQWs for Structure C, disregarding the reduced electron kinetic energy. Nevertheless, the ambiguity can be further clarified by showing Figure 5b. Figure 5b illustrates that, in spite of the highest Si doping concentration in the X region for the n-Al<sub>0.60</sub>Ga<sub>0.40</sub>N layer, the electron leakage level for Structure C is the smallest among the three investigated DUV LEDs. The suppressed electron leakage level was exactly due to the deceleration effect to the electrons in the n-AlGaN layer [14]. Because the electrons cannot lose adequate energy in the X region for Structure A, the largest electron leakage level was observed in the hole supplier layer, according to Figure 5b. Although Structure C yields the smallest electron leakage current, the optical output power decreases, according to Figure 3.

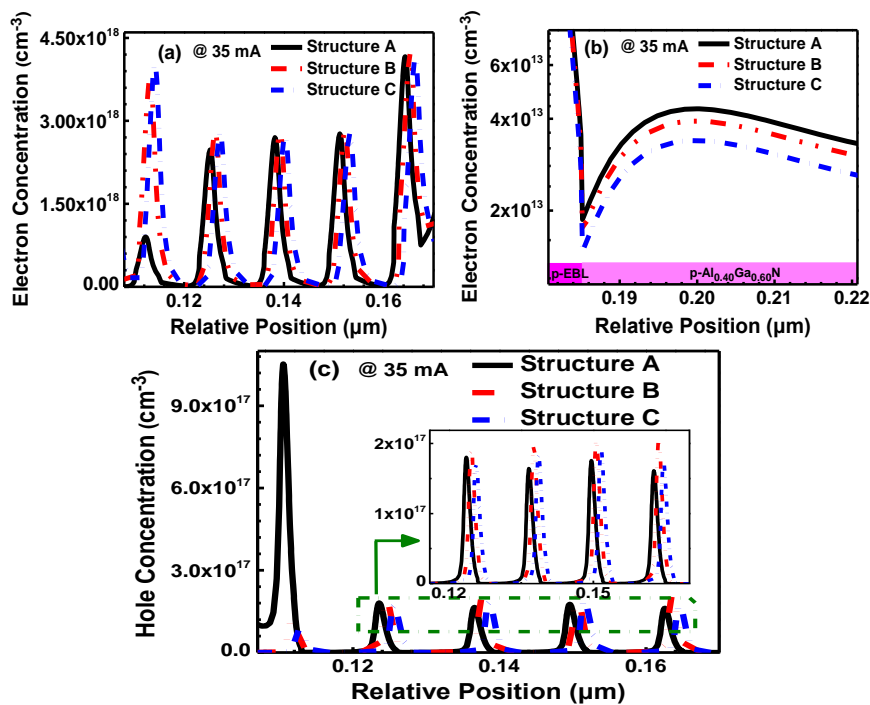


**Figure 5.** Electron concentration profiles (a) in the MQWs; (b) in the hole supplier layers; and (c) hole concentration profiles in the MQWs for Structures A, B, and C, respectively. Data are collected at the injection current level of 35 mA.

To examine the origins for the observed decrease in the optical output power for Structure C, as compared with that for Structure B in Figure 3, we show, in Figure 5c, the hole distribution in the MQWs for the three structures. Although both Structure B and Structure C have a smaller hole concentration than Structure A in the first quantum well (QW), the hole distribution across the MQWs for Structure B and Structure C were more uniform, with Structure B possessing the highest hole concentration, addressing the observed highest optical output power for Structure B. Note, the hole concentration in the first quantum well for Structure A was the largest, which is because of the fact that the smaller Si doping concentration in the “X region” produced fewer ionized Si<sup>+</sup> dopants to compensate for the polarization induced negative charges at the n-Al<sub>0.60</sub>Ga<sub>0.50</sub>N/Al<sub>0.55</sub>Ga<sub>0.45</sub>N interface. This results in less hole depletion in the first quantum well when compared with Structures B and C.

Figure 6 presents the radiative recombination rate in the MQWs at the current of 35 mA for the three DUV LEDs. It is apparent from Figure 6 that Structure B was better than the other two structures in the overall radiative recombination rate. The poorest overall radiative recombination rate was given by Structure A. These results agree well with the optical output power in Figure 3. Please note that, although Structure C was beneficial for enhancing the electron injection efficiency, the hole concentration in the MQWs of Structure C was smaller than that of Structure B from Figure 5c, leading to a lower radiative recombination rate when compared with Structure B.

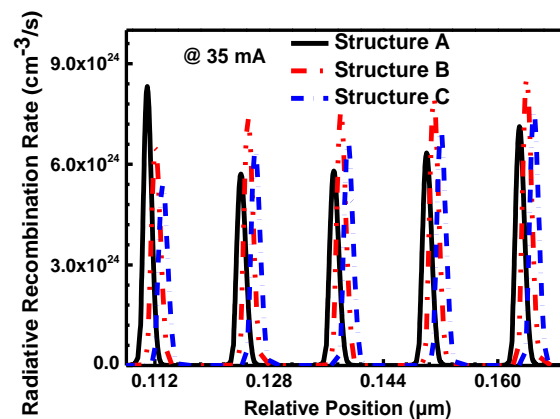


**Figure 6.** Radiative recombination rate in the MQWs for Structures A, B, and C, respectively. Data are collected at the injection current level of 35 mA.

#### 4. Conclusions

In summary, we reveal that different Si doping concentrations in the n-Al<sub>0.60</sub>Ga<sub>0.40</sub>N layer can influence the electric field intensity for [0001] oriented DUV LEDs. According to our study, the electric field intensity in the n-Al<sub>0.60</sub>Ga<sub>0.40</sub>N layer can become large by increasing the Si doping concentration level. The large electric field intensity can reduce the kinetic energy for the free electrons, which then helps to improve the electron injection efficiency for the MQW region. However, excessive Si doping concentration obstructs the hole transport. Therefore, it is important to optimize the Si doping concentration in the n-Al<sub>0.60</sub>Ga<sub>0.40</sub>N layer to effectively enhance the optical output power. We believe the proposed approach and the physical concept are very useful for the community to further understand the device physics and enhance the quantum efficiency for DUV LEDs.

**Author Contributions:** M.F., Z.-H.Z. and W.B. designed the device structures, set up the physical models and co-wrote the manuscript. C.C., K.T. and Y.Z. co-wrote the manuscript. All authors read and approved the final manuscript.

**Funding:** The authors acknowledge the support by the National Key R&D Program of China (Program Nos. 2016YFB0400800, 2016YFB0400801), Natural Science Foundation of Hebei Province (Project No. F2018202080), National Natural Science Foundation of China (Project Nos. 51502074, 61604051), Technology Foundation for Selected Overseas Chinese Scholar by Ministry of Human Resources and Social Security of the People's Republic of China (Project No. CG2016008001).

**Conflicts of Interest:** The authors declare no conflict of interest.

#### References

1. Kneissl, M. *A Brief Review of III-Nitride UV Emitter Technologies and Their Application*; Springer International Publishing: Cham, Switzerland, 2015; Volume 227, pp. 1–25.
2. Sun, J.; Sun, H.; Yi, X.; Yang, X.; Liu, T.; Wang, X.; Zhang, X.; Fan, X.; Zhang, Z.; Guo, Z. Efficiency enhancement in AlGaIn deep ultraviolet light emitting diodes by adjusting Mg doped staggered barriers. *Superlattices Microstruct.* **2017**, *107*, 49–55. [[CrossRef](#)]
3. Ji, X.; Yan, J.; Guo, Y.; Sun, L.; Wei, T.; Zhang, Y.; Wang, J.; Yang, F.; Li, J. Tailoring of Energy Band in Electron-Blocking Structure Enhancing the Efficiency of AlGaIn-based Deep Ultraviolet Light-Emitting Diodes. *IEEE Photonics J.* **2016**, *8*, 1600607. [[CrossRef](#)]
4. Zhang, Z.-H.; Ju, Z.; Liu, W.; Tan, S.T.; Ji, Y.; Kyaw, Z.; Zhang, X.; Hasanov, N.; Sun, X.W.; Demir, H.V. Improving hole injection efficiency by manipulating the hole transport mechanism through p-type electron blocking layer engineering. *Opt. Lett.* **2014**, *39*, 2483–2486. [[CrossRef](#)] [[PubMed](#)]
5. Ji, Y.; Zhang, Z.-H.; Tan, S.T.; Ju, Z.G.; Kyaw, Z.; Hasanov, N.; Liu, W.; Sun, X.W.; Demir, H.V. Enhanced hole transport in InGaIn/GaN multiple quantum well light-emitting diodes with a p-type doped quantum barrier. *Opt. Lett.* **2013**, *38*, 202–204. [[CrossRef](#)] [[PubMed](#)]

6. Zhang, Y.; Yu, L.; Li, K.; Pi, H.; Diao, J.; Wang, X.; Shen, Y.; Zhang, C.; Hu, W.; Song, W.; et al. The improvement of deep-ultraviolet light-emitting diodes with gradually decreasing Al content in AlGa<sub>N</sub> electron blocking layers. *Superlattices Microstruct.* **2015**, *82*, 151–157. [[CrossRef](#)]
7. Huang, J.; Guo, Z.; Guo, M.; Liu, Y.; Yao, S.; Sun, J.; Sun, H. Study of Deep Ultraviolet Light-Emitting Diodes with a p-AlInN/AlGa<sub>N</sub> Superlattice Electron-Blocking Layer. *J. Electron. Mater.* **2017**, *46*, 4527–4531. [[CrossRef](#)]
8. Kuo, Y.-K.; Chen, F.-M.; Lin, B.-C.; Chang, J.-Y.; Shih, Y.-H.; Kuo, H.-C. Simulation and Experimental Study on Barrier Thickness of Superlattice Electron Blocking Layer in Near-Ultraviolet Light-Emitting Diodes. *IEEE J. Quantum Electron.* **2016**, *52*, 3300306. [[CrossRef](#)]
9. Lin, Y.-Y.; Chuang, R.W.; Chang, S.-J.; Li, S.; Jiao, Z.-Y.; Ko, T.-K.; Hon, S.J.; Liu, C.H. GaN-Based LEDs with a Chirped Multiquantum Barrier Structure. *IEEE Photonics Technol. Lett.* **2012**, *24*, 1600–1602. [[CrossRef](#)]
10. Tsai, M.-C.; Yen, S.-H.; Kuo, Y.-K. Deep-ultraviolet light-emitting diodes with gradually increased barrier thicknesses from n-layers to p-layers. *Appl. Phys. Lett.* **2011**, *98*, 111114. [[CrossRef](#)]
11. Bao, X.; Sun, P.; Liu, S.; Ye, C.; Li, S.; Kang, J. Performance improvements for AlGa<sub>N</sub>-based deep ultraviolet light-emitting diodes with the p-type and thickened last quantum barrier. *IEEE Photonics J.* **2015**, *7*, 1400110. [[CrossRef](#)]
12. Guo, W.; Xu, F.; Sun, Y.; Lu, L.; Qin, Z.; Yu, T.; Wang, X.; Shen, B. Performance improvement of AlGa<sub>N</sub>-based deep-ultraviolet light-emitting diodes by inserting single spike barriers. *Superlattices Microstruct.* **2016**, *100*, 941–946. [[CrossRef](#)]
13. Zhang, Z.-H.; Liu, W.; Tan, S.T.; Ju, Z.; Ji, Y.; Kyaw, Z.; Zhang, X.; Hasanov, N.; Zhu, B.; Lu, S.; et al. On the mechanisms of InGa<sub>N</sub> electron cooler in InGa<sub>N</sub>/Ga<sub>N</sub> light-emitting diodes. *Opt. Express* **2014**, *22*, A779–A789. [[CrossRef](#)] [[PubMed](#)]
14. Zhang, Z.-H.; Ji, Y.; Liu, W.; Tan, S.T.; Kyaw, Z.; Ju, Z.; Zhang, X.; Hasanov, N.; Lu, S.; Zhang, Y.; et al. On the origin of the electron blocking effect by an n-type AlGa<sub>N</sub> electron blocking layer. *Appl. Phys. Lett.* **2014**, *104*, 073511. [[CrossRef](#)]
15. Tian, K.; Chen, Q.; Chu, C.; Fang, M.; Li, L.; Zhang, Y.; Bi, W.; Chen, C.; Zhang, Z.-H.; Dai, J. Investigations on AlGa<sub>N</sub>-based deep-ultraviolet light-emitting diodes with Si-doped quantum barriers of different doping concentrations. *Phys. Status Solidi* **2018**, *12*, 1700346. [[CrossRef](#)]
16. Ryu, H.-Y.; Jeon, K.-S.; Kang, M.-G.; Choi, Y.; Lee, J.-S. Dependence of efficiencies in Ga<sub>N</sub>-based vertical blue light-emitting diodes on the thickness and doping concentration of the n-Ga<sub>N</sub> layer. *Opt. Express* **2013**, *21*, A190–A200. [[CrossRef](#)] [[PubMed](#)]
17. Lee, J.-H.; Han, S.-H.; Song, K.-R.; Lee, S.-N. Optical and electrical improvements of semipolar (11-22) Ga<sub>N</sub>-based light emitting diodes by Si doping of n-Ga<sub>N</sub> template. *J. Alloys Compd.* **2014**, *598*, 85. [[CrossRef](#)]
18. Fiorentini, V.; Bernardini, F.; Ambacher, O. Evidence for nonlinear macroscopic polarization in III–V nitride alloy heterostructures. *Appl. Phys. Lett.* **2002**, *80*, 1204–1206. [[CrossRef](#)]
19. Kuo, Y.-K.; Chang, J.-Y.; Chen, F.-M.; Shih, Y.-H.; Chang, H.-T. Numerical Investigation on the Carrier Transport Characteristics of AlGa<sub>N</sub> Deep-UV Light-Emitting Diodes. *IEEE J. Quantum Electron.* **2016**, *52*, 3300105. [[CrossRef](#)]
20. Piprek, J. Efficiency droop in nitride-based light-emitting diodes. *Phys. Status Solidi* **2010**, *207*, 2217–2225. [[CrossRef](#)]
21. Schubert, E.F. *Light-Emitting Diodes*; Cambridge University Press: Cambridge, UK, 2006; p. 104. ISBN 9780521865388.
22. Hang, D.R.; Liang, C.-T.; Huang, C.F.; Chang, Y.H.; Chen, Y.F.; Jiang, H.X.; Lin, J.Y. Effective mass of two-dimensional electron gas in an Al<sub>0.2</sub>Ga<sub>0.8</sub>N/Ga<sub>N</sub> heterojunction. *Appl. Phys. Lett.* **2001**, *79*, 66–68. [[CrossRef](#)]
23. Vurgaftman, I.; Meyer, J.R. Band parameters for nitrogen-containing semiconductors. *J. Appl. Phys.* **2003**, *94*, 3675. [[CrossRef](#)]

